AD-A038 358 AIR FORCE WEAPONS LAB KIRTLAND AFB N MEX F/G 20/5
IMPROVED SURFACE DAMAGE BY RADIO-FREQUENCY SPUTTERED OVERCOATIN--ETC(U)
MAR 77 J R BETTIS
UNCLASSIFIED AFWL-TR-76-58 NL

| OF |
AD
A038358

END

DATE
FILMED
5 - 77

AFWL-TR-76-58

AFWL-TR-
76-58

IMPROVED SURFACE DAMAGE BY RADIO-FREQUENCY SPUTTERED OVERCOATING

March 1977

Final Report

Approved for public release; distribution unlimited.

AIR FORCE WEAPONS LABORATORY
Air Force Systems Command
Kirtland Air Force Base, NM 87117

This final report was prepared by the Air Force Weapons Laboratory, Kirtland Air Force Base, New Mexico, under Job Order ILIR7406. Major Jerry R. Bettis (LRE) was the Laboratory Project Officer-in-Charge.

When US Government drawings, specifications, or other data are used for any purpose other than a definitely related Government procurement operation, the Government thereby incurs no responsibility nor any obligation whatsoever, and the fact that the Government may have formulated, furnished, or in any way supplied the said drawings, specifications, or other data is not to be regarded by implication or otherwise as in any manner licensing the holder or any other person or corporation or conveying any rights or permission to manufacture, use, or sell any patented invention that may in any way be related thereto.

This report has been reviewed by the Information Office (OI) and is releasable to the National Technical Information Service (NTIS). At NTIS, it will be available to the general public, including foreign nations.

This technical report has been reviewed and is approved for publication.

JERRY R. BETTIS
Major, USAF
Project Officer

FOR THE COMMANDER

RONALD F. PRATER
Lt Colonel, USAF
Chief, Short Range Beam Control Branch

DEMOS T. KYRAZIS
Colonel, USAF
Chief, Laser Development Division

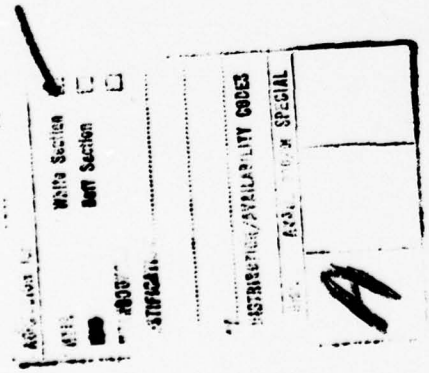

DO NOT RETURN THIS COPY. RETAIN OR DESTROY.

UNCLASSIFIED

SECURITY CLASSIFICATION OF THIS PAGE (When Data Entered)

REPORT DOCUMENTATION PAGE	READ INSTRUCTIONS BEFORE COMPLETING FORM
1. AFWL-TR-76-58	2. GOVT ACCESSION NO. 3. RECIPIENT'S CATALOG NUMBER
4. TITLE (and Subtitle) IMPROVED SURFACE DAMAGE BY RADIO-FREQUENCY SPUTTERED OVERCOATING	5. TYPE OF REPORT & PERIOD COVERED Final Report.
	6. PERFORMING ORG. REPORT NUMBER
7. AUTHOR(s) Jerry R. Bettis, Major, USAF	8. CONTRACT OR GRANT NUMBER(s)
9. PERFORMING ORGANIZATION NAME AND ADDRESS Air Force Weapons Laboratory (LRE) Kirtland Air Force Base, NM 87117	10. PROGRAM ELEMENT, PROJECT, TASK AREA & WORK UNIT NUMBERS 62601F/ILIR7406
11. CONTROLLING OFFICE NAME AND ADDRESS	12. REPORT DATE March 1977
	13. NUMBER OF PAGES 35
14. MONITORING AGENCY NAME & ADDRESS (if different from Controlling Office) 34 p. ILIR	15. SECURITY CLASS. (of this report) UNCLASSIFIED
	15a. DECLASSIFICATION/DOWNGRADING SCHEDULE

16. DISTRIBUTION STATEMENT (of this Report)

Approved for public release; distribution unlimited.

74

17. DISTRIBUTION STATEMENT (of the abstract entered in Block 20, if different from Report)

18. SUPPLEMENTARY NOTES

19. KEY WORDS (Continue on reverse side if necessary and identify by block number)

Laser Damage	Laser-Induced	Dielectrics
Thin Films	Radiation	Films
Damage	Interaction	Radio Frequency Sputtering
Laser	Fluorides	

20. ABSTRACT (Continue on reverse side if necessary and identify by block number)

Ten dielectric materials were deposited in half-wavelength optically thick films on dielectric substrate with varying surface roughness. The films were subjected to damaging radiation from a TEM_{00} ND^{+3} in glass laser operating at 1.06 μm. The threshold optical field for damage was determined for each film. It was demonstrated that substrate roughness was an overriding consideration in the thin-film thresholds and that no masking of defects by the film was exhibited.

TEM mode ND(+3)

micrometers

DD FORM 1 JAN 73 1473 EDITION OF 1 NOV 65 IS OBSOLETE

UNCLASSIFIED

SECURITY CLASSIFICATION OF THIS PAGE (When Data Entered)

013150

CONTENTS

Section		Page
I	INTRODUCTION	5
	Sample Preparation	5
	Surface Characterization	7
II	EXPERIMENT	14
	Active Diagnostics	17
III	RESULTS	20
	Raw Data	20
	Data Reduction: The energy threshold	20
	Data Reduction: The electric field threshold	22
	Data Reduction: Accuracy of results	23
	Results of the Current Study: Thin films	23
IV	CONCLUSIONS	31
	REFERENCES	32

ILLUSTRATIONS

Figure		Page
1	Schematic Representation of Fringes of Equal Chromatic Order (FECO) Interferometric Method for Determining Surface Roughness	8
2	Schematic Representation of the Total Integrated Scatter (TIS) Method for Determining Surface Roughness	9
3	Reflection Spectra of Two Half-Wave Homogeneous Films Compared to the Fused Silica Substrate. Reflectance is on a Relative Scale	11
4	Reflection Spectra of Two Half-Wave Inhomogeneous Films Compared to the Fused Silica Substrate. Reflectance is on a Relative Scale	12
5	Computed Reflectance Spectrum of a Four-Film, Half-Wave Stack With Indexes 1.28, 1.32, 1.36, and 1.38 Increasing Outward From a 1.45 Index Substrate	13
6	Experimental Arrangement	15
7	Method Used to Determine Energy Threshold for Damage	21

TABLES

Table		Page
1	Thin-film Threshold Vs. Predicted Bare-surface Threshold	25
2	Ratio of Thin-film to Bare-surface Threshold	25
3	Threshold of Film Stacks	27
4	Thresholds for MgF_2 Films Vs. Deposition Technique	27
5	Damage Thresholds for $\lambda/2$ Films Vs. OH^-	28
6	Threshold Vs. Roughness for the SiO_2-Overcoated Samples	29
7	Threshold Vs. Roughness for the MgF_2-Overcoated Samples	30

SECTION I. INTRODUCTION

Transparent optical elements intended for use in high-peak power laser systems can suffer failure under irradiation by the laser. Due primarily to mechanical and material imperfections, the surfaces of the transparent elements are the most susceptible to laser-induced damage. The very processes which are intended to produce optical quality surfaces may contribute to the failure of the surfaces. Grinding and polishing may imbed particulate matter into the surface, which absorbs laser radiation and leads to damage. Polishing by conventional means cannot eliminate microcracks and fissures that contribute to a lowering of the threshold power density for laser-induced damage. Other polishing and finishing techniques such as etching, ion polishing, bowl-feed or superpolishing, and flame polishing do appear to raise the damage threshold. However, these processes are either very expensive, time-consuming, or not presently controllable to the point of being quantitative. The purpose of this research effort was to determine whether the microcracks and fissures present on the surfaces of conventionally finished optics could be successfully masked by a half-wavelength thick film to such an extent that an increase in damage threshold over a bare surface would accrue.

To test this conjecture 10 different dielectric materials were placed in half-wavelength thick films onto transparent substrates consisting of four different materials. The film/substrates were then subjected to damaging radiation from a TEM_{oo} mode Nd^{+3} in glass laser operating at 1.06 μm wavelength with 40 nanosecond pulse duration. The results were compared to damage testing data taken on the uncoated substrate materials.

Sample Preparation

The test samples for this study required surface finishes of two types: (1) bare surfaces and substrate surfaces for film depositions with the lowest practical surface roughness and (2) bare surfaces and substrate surfaces for film depositions with a controlled range of surface roughnesses. The latter category was designed to test the influence of surface roughness on the laser-induced damage threshold and whether thin-film thresholds are affected by the surface roughness of the substrate. Both the smooth and rough surfaces were created by variations of the process of controlled grinding.

The effect of the grinding process in the preparation of optical surfaces extends below the surface. A layer of sub-surface disorder in the form of microcracks and fissures develops when an optical surface is ground. A commonly accepted rule in the optical industry is that subsurface disorder extends to a depth roughly three times the diameter of the grit used in the grinding process (ref. 1). Controlled grinding is a technique for minimizing the subsurface disorder. The controlled grinding process used to obtain the "best finish" surface proceeds as follows: A 30 μm grit is used to rough in the surface finish. Since this process introduces a subsurface disorder to a depth of ∿90 μm, the next stage, employing 20 μm grit, proceeds until ∿100 μm of the material is removed, thus eliminating the disorderly effect of the 30 μm grit. This process continues through 12, 5, and 3 μm diameter alumina grit, each stage removing material to a depth about three times the diameter of the previous grit. The surface is then polished, which removes about 10 μm of material and gives the final finish. The final roughness values varied from about 10 Å rms for fused silica to about 40 to 50 Å for sapphire and ZnS.

The roughness samples were created by interrupting the polising at selected total polish times. Samples in the 300 Å rms range were polished for about 30 minutes. Forty minutes of polishing time gave a 150 Å rms surface, while 10 to 20 hours gave 40 to 50 Å rms, and the best finish (less than 20 Å rms) required 40 hours polishing time.

The dielectric films were deposited by one of three frequently employed techniques: rf sputtering, electron beam heating, and thermal-evaporation. A set of MgF_2 samples were prepared by each of the three deposition techniques. The MgF_2 films applied to substrates on which the substrate roughness was varied were deposited by thermal evaporation. The remainder of the films were applied by electron beam heating.

Each dielectric film was specified to be a half wave in optical thickness at the 1.06 μm wavelength used in the study. This parameter was monitored by observing the reflectance of the film-substrate system as the film was being applied. For films whose index is greater than the substrate index a minimum in reflectance is obtained when a half wave optical thickness is reached. For homogeneous films this minimum corresponds to the reflectance of the bare substrate. The half wave thickness was chosen because this assured that the electric field at the substrate-film interface was the same as the optical electric field at the film-air interface. It was also the thickness which gave the least variation

in the electric field of a standing wave pattern for slight variations in the thickness. For films whose index is less than the index of the substrate, a reflectance maximum is obtained when a half wave optical thickness is reached.

Surface Characterization

One of the prime reasons for conducting this study was to determine those characteristics of surface finish and film deposition which materially affect the laser-induced surface threshold. It was imperative, therefore, to fully characterize the surfaces of both the uncoated samples and the thin-film coatings.

The surfaces were measured for roughness by three methods: fringes of equal chromatic order (FECO), total integrated scatter (TIS), and Talystep depth profiling. FECO was the prime indicator of surface roughness while the total integrated scatter and Talystep were used only as auxiliary measurements. For a flat surface the roughness is defined as the root mean square deviation of surface heights from the average surface. Thus on a surface with a specified rms roughness surface, features as large as twice that in depth are not uncommon.

FECO interferometry is a technique shown schematically in figure 1. Both a reference flat and the surface to be measured are partially silvered. The sample and flat are brought to within a wavelength or so of each other and parallel. A portion of the two plates is imaged by lens L_2 onto the slit of a spectroscope. As the distance between the flat and sample varies due to surface roughness, the spectroscope passes only those wavelengths which satisfy $2d = m\lambda$ (m is an integer). Since m is constant along any one fringe, d/λ is constant. The fringes, referred to as fringes of equal chromatic order, reveal the topographical features of the surface of the sample imaged on the slit of the spectroscope (refs. 2 and 3).

Total integrated scatter, from a discussion by Porteus (ref. 4), is a technique which relates the scatter from the reflection of a laser beam incident on a surface to the surface roughness. The sample is normally located tangent to one port of a hollow, diffuse reflecting sphere. Laser light enters another port and the nonspectral reflected light enters a detector after being totally integrated by the sphere (figure 2). Surface roughness is given by

$$\sigma = \frac{\lambda}{4\pi} \sqrt{-\ell n(1-TIS)} \qquad (1)$$

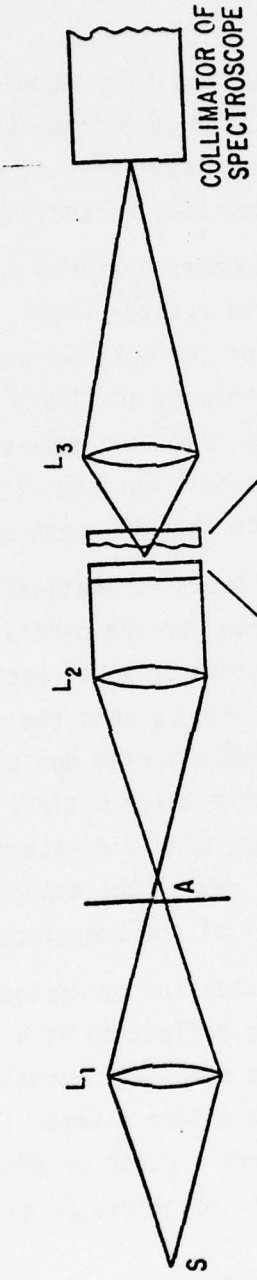

Figure 1. Schematic Representation of Fringes of Equal Chromatic Order (FECO) Interferometric Method for Determining Surface Roughness.

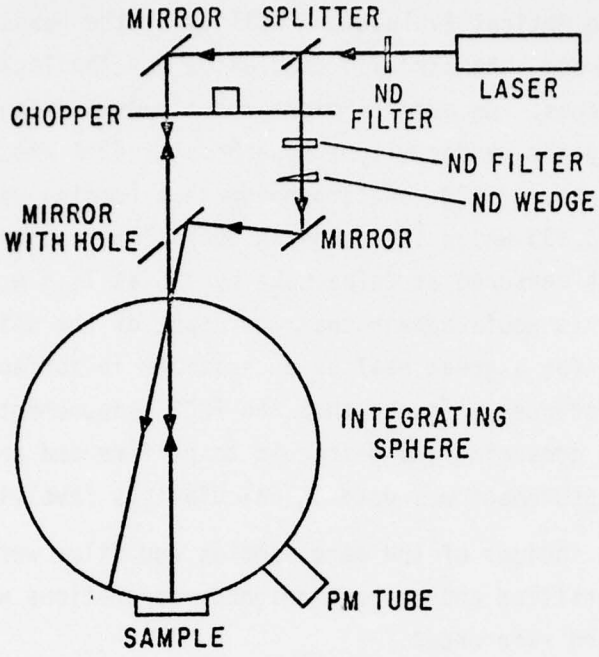

Figure 2. Schematic Representation of the Total Integrated Scatter (TIS) Method for Determining Surface Roughness.

where λ is the wavelength of the test laser and TIS is the fraction of the test beam scattered outside the prime spectral reflection. The technique also affords a method for determining scatter of imperfections in thin film coatings.

The Talystep device uses a weighted stylus and electronic amplification of its vertical motion to topographically scan the surface of the sample. For hard films it can also be used to mechanically measure the physical thickness of the film. The final method was reliable for surfaces with values of $\sigma > \sim 50 - 75$ Å rms, but the diameter of the tip of the stylus precluded the measurement of very small features and gave uniformly too low readings on the smoother samples. The smallest stylus radius was 1.0 μm. To obtain an rms surface roughness by Talystep, a one-dimensional scan of 2 mm in length is obtained at several representative locations. For each scan of the topography of the surface, the surface height is measured from a baseline at regular intervals to determine an average surface height. The deviation of the surface height from the average is then measured at regular intervals, and the root mean square deviation is calculated. It is this deviation which is termed surface roughness.

From the results of surface roughness measurements performed by the vendor, the author, and the Optical Evaluation Facility at the Naval Weapons Center, China Lake, California, the striking conclusion was the lack of correlation between the measurements. An example might prove enlightening. Sample 800-7169-080 was supplied by the vendor with a roughness of 42 Å rms as determined by the most accurate technique, FECO. Accompanying that reading was the total integrated scatter of 0.11% which indicates an equivalent roughness of 16.7 Å rms. The same sample was measured at China Lake by TIS at 16.5 Å and by the author by Talystep as 27 Å. It would appear that the state of the art in surface measurements still allows for a great deal of uncertainty in surface roughness determinations. Industry sources indicate that the FECO measurement is the most reliable, although very time consuming and difficult to perform and analyze. For this reason the FECO measurement was used in calculations involving surface roughness.

The refractive indices of the bare samples and films were measured by ellipsometry. Number densities and nearest neighbor separations were calculated or obtained from standard references.

Of major concern in the study of the thin films was the homogeneity of the film throughout its depth. The spectral reflectivity is a reliable indicator of this parameter. A Carey 14 spectrophotometer was used in the double pass reflection mode to obtain the spectral reflectivity of the films. Figure 3 is the spectral response of two $\lambda/2$ ThF_4 and ZrO_2 films. These two films are examples of the excellence of a film coater's art in being able to produce homogeneous coatings. Since both films were specified as half wave at 1.06 μm, a perfect film would have the reflectance of the substrate at 1.06 μm. Since ThF_4, at n = 1.49, matches its index more closely with the fused silica substrate index at 1.449 than does the ZrO_2 at n = 2.0, the reflectance of the ThF_4 film versus wavelength is not very different from the substrate. In fact the maximum reflectance of the ThF_4 film on SiO_2 at 2.12 μm, where the film is a quarter wavelength thick, is only 4.15% compared to 3.36% for the substrate while for the ZrO_2 film the maximum is 22.3% at 2.12 μm. Conversely, figure 4 reveals the spectral response of LiF and MgF_2. These films display a markedly inhomogeneous character with an index apparently increasing outward from the substrate. Since they both have refractive indexes less than that of the substrate, their reflectance should increase toward and match that of the substrate at 1.06 μm. These two films along with BaF_2 exhibited the most inhomogeneity in this respect. The author will call attention to this fact during the discussion of the thin-film results.

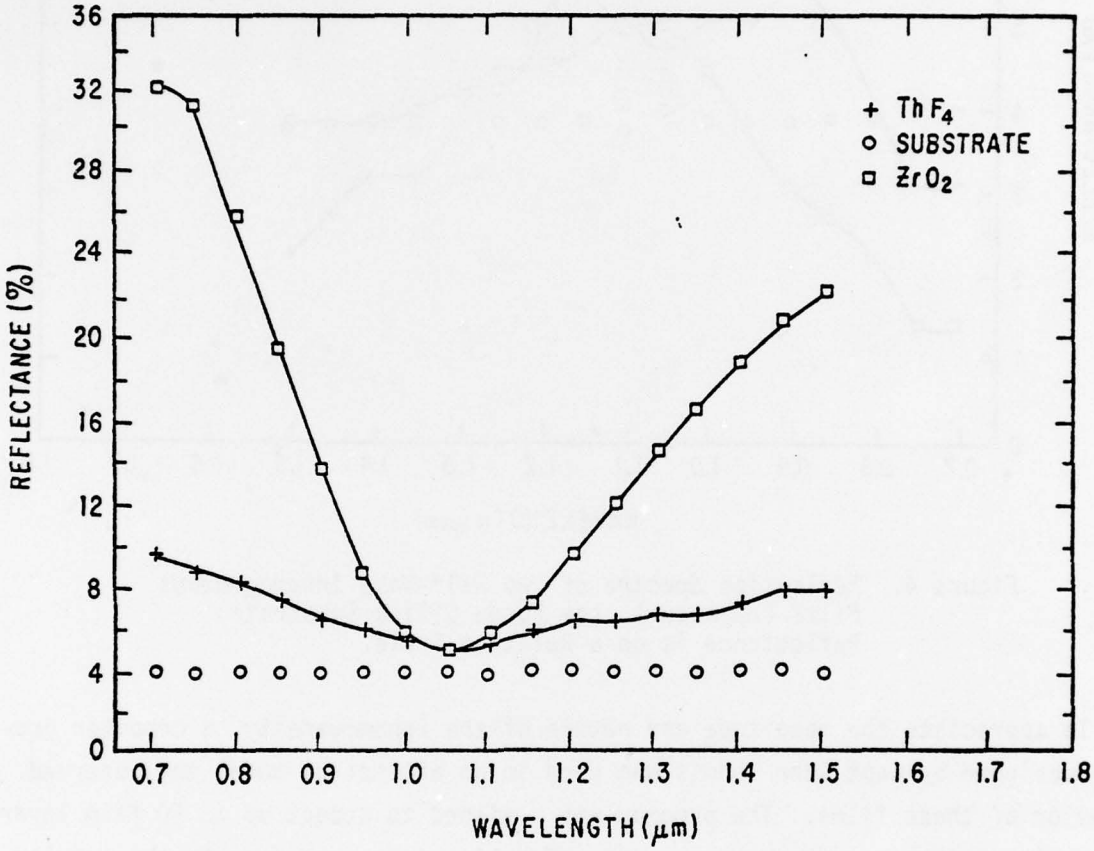

Figure 3. Reflection Spectra of Two Half-Wave Homogeneous Films Compared to the Fused Silica Substrate. Reflectance is on a Relative Scale.

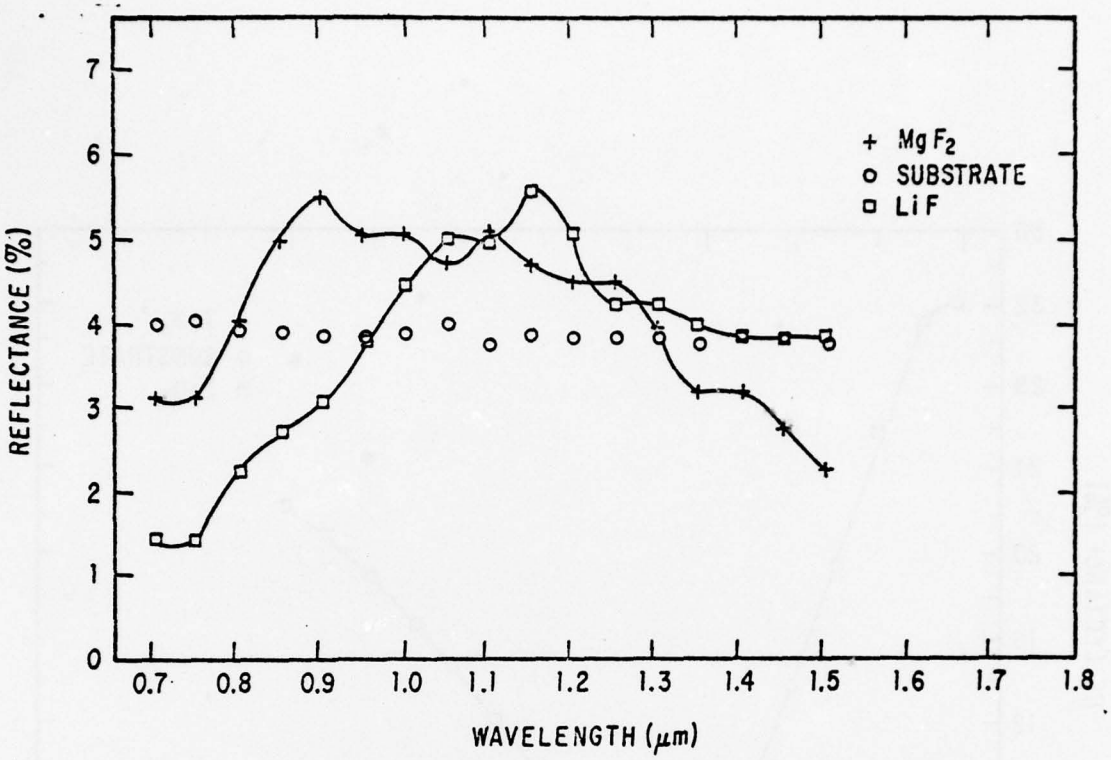

Figure 4. Reflection Spectra of Two Half-Wave Inhomogeneous Films Compared to the Fused Silica Substrate. Reflectance is on a Relative Scale.

To appreciate the magnitude and nature of the inhomogeneity, a computer program designed by Capt John Loomis was used in an attempt to model the observed behavior of these films. The program was designed to accept up to 50 film layers of varying thickness, absorptance, and refractive index and compute the angular and wavelength dependence of the reflectance. The parameters used included the total physical thickness of the film as measured by Talystep, the refractive index of the substrate, and the measured refractive index at the surface of the film. The inhomogeneous film with varying index was discretized into a stack of from four to eight films with refractive index and thickness the variable parameters. It was found that a variation in the refractive index of about 7% (1.28 at the substrate to 1.38 at the film surface) produced a spectral response quite suggestive of the measured spectral response. One result has been reproduced as figure 5, which should be compared to figure 4.

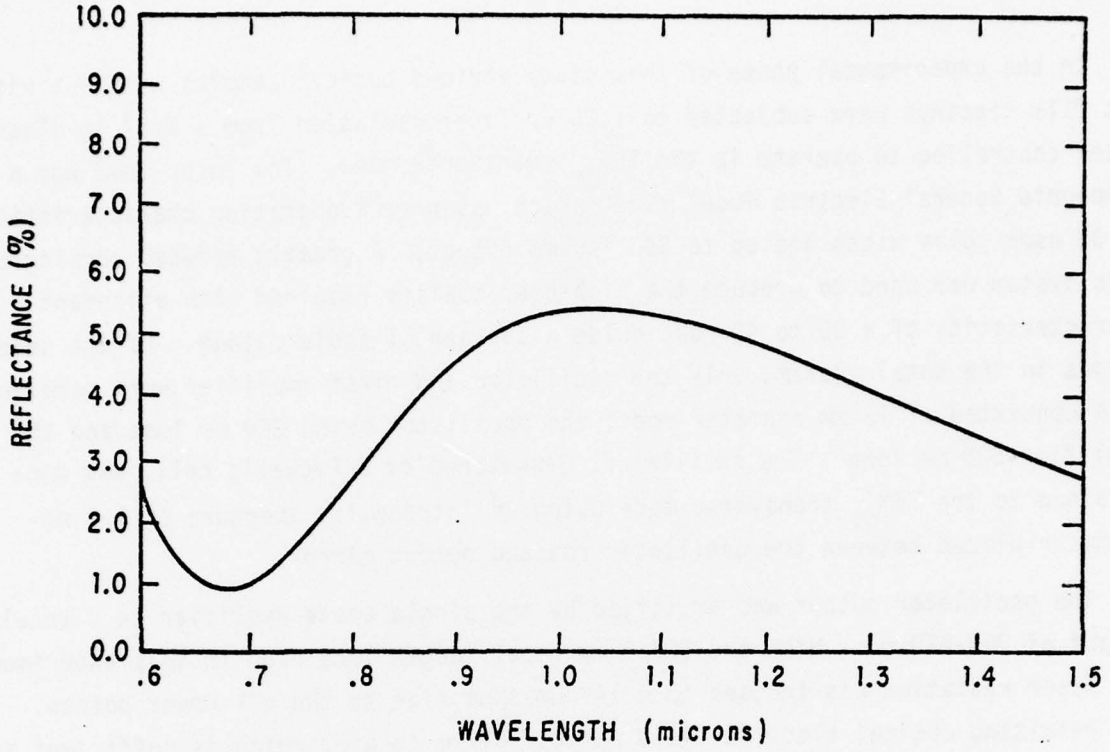

Figure 5. Computed Reflectance Spectrum of a Four-Film, Half-Wave Stack With Indexes 1.28, 1.32, 1.36, and 1.38 Increasing Outward From a 1.45 Index Substrate.

If one assumes that fused silica is invariant, independent of the source, a comparison of the absorption and transmission spectra for various fused silica blanks will quickly dispel that notion. While the major portion of this effort used fused silica supplied by the Amersil Corporation under the trade name Optosil I, an ancillary study involved fused silica substrates supplied by a variety of manufacturers. During the coating process absorption spectra are routinely taken. From these spectra varying amounts of hydroxyl ion were identified in the different fused silica types. This observation formed the basis for an unexpected conclusion which at first seemed to be anomalous behavior. This result will be discussed in detail later. This last measurement was mentioned to indicate that in thin-film coatings it is not at all entirely obvious what deposition condition, techniques and properties of films lead to high damage threshold films.

SECTION II
EXPERIMENT

In the experimental phase of this study various optical samples with and without film coatings were subjected to 1.06 μm laser radiation from a Nd^{+3} in glass laser controlled to operate in the TEM_{oo} transverse mode. The laser used was a Compagnie General Electric Model VD640 which has normal operating characteristics of 35 nsec pulse width and up to 500 joules output. A greatly reduced version of this system was used to produce the high beam quality required with attendant characteristics of a 30 to 40 nsec pulse width and ∿1 joule output. Of the seven stages in the total system, only the oscillator and first amplifier were retained. Each consisted of 16 mm diameter rods; the oscillator being 300 mm long and the amplifier 500 mm long . The oscillator, Q-switched by a Pockel's cell, was constrained to the TEM_{oo} transverse mode using an intracavity aperture of 1.9 mm diameter placed between the oscillator rod and output mirror.

The oscillator output was amplified by the single state amplifier to a total output of 380-410 mJ. With the 503.5 mm focal length lens used in this experiment, the laser radiation was focused to a 147 μm spot size to the e^{-2} power points. The resulting optical electric field was 6.7 MV/cm in air, which is sufficient to damage the surface and bulk of most conventional dielectrics in a 30 to 40 nsec pulse.

The remainder of the equipment was used for diagnostics and parameterization.

Figure 6 is a schematic diagram of the optical test conditions. The laser beam was directed down an optical bench with the aid of two 45° - 100% reflectors. These reflectors were gimbal mounted to facilitate alignment of the system. The samples were held in a translating-rotatable mount approximately 12 meters from the beam waist of the oscillator.

The focusing and beam attenuation systems were mounted on a two-meter lathe bed optical bench. This bench was rigidly attached to a 4 inch thick honeycomb-backed steel plate for stability.

The focusing lens was a carefully selected biconvex fused silica lens of the highest quality. The lens chosen, 503.5 mm focal length, was tested along with a couple of dozen other candidates with a Foucault knife edge device. The chosen lens alone showed excellent sphericity.

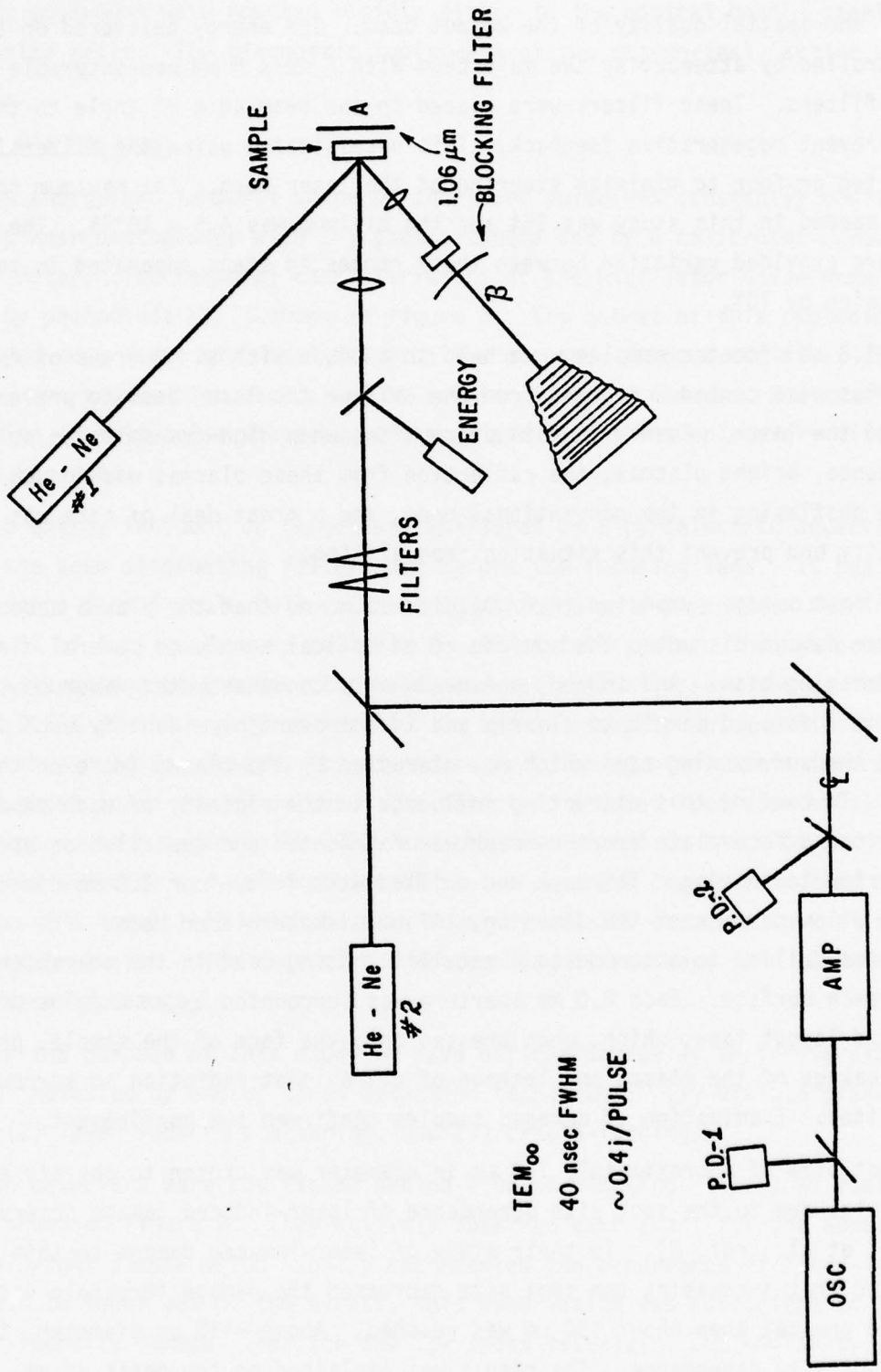

Figure 6. Experimental Arrangement.

The laser was operated at constant input energy in order to maintain the temporal and spatial quality of the output beam. The energy delivered on target was controlled by attenuating the main beam with 5 mm x 5 mm non-saturable Schott optical filters. These filters were placed in the beam at a 6° angle to the normal to prevent regenerative feedback. This necessitated using the filters in sets of two or four to minimize steering of the laser beam. The maximum transmission needed in this study was 35% and the minimum was 4.5×10^{-2}%. The set of 64 filters provided variation between these ranges in steps separated in total transmission by 10%.

The 3.8 cm diameter samples were held in a mount with six degrees of freedom. The samples were canted 5 degrees from the axis of the laser beam to prevent feedback into the laser. Even with this precaution, when high-transmission pulses caused dense, bright plasmas, the reflection from these plasmas was enough to generate postlasing in the conventional mode, and a great deal of care was taken to identify and prevent this situation from arising.

In a past damage symposium (ref. 7), it was noted that the plasma associated with laser damage disrupted the surface of an optical sample to several diameters of the damaging beam. And indeed, one needs only condense water vapor on the surface of a damaged sample to clearly and incontrovertibly identify each damage site and the surrounding area which was disrupted by the plasma (more on this to follow). To confine this disrupting influence to the vicinity of each separate damage site, a face-plate aperture mask was fabricated and installed on each sample prior to testing. The mask was drilled with fifty-four 2.0 mm diameter holes to allow passage of the damaging, 147 μm diameter laser beam. The center 1.25 cm was drilled to accommodate a metallic coating used in the characterization of each surface. Each 2.0 mm aperture was surrounded by an annulus of circuit board layout tape, which, when pressed onto the face of the sample, prevented leakage of the plasma and leakage of ultraviolet radiation to surrounding damage sites. Examination of damaged samples confirmed the confinement.

A spot size of approximately 150 μm in diameter was chosen to obviate erroneous results due to the spot size dependence of laser-induced damage observed by DeShazer, et al. (ref. 8). In their study of laser-induced damage to thin films, they noted that increasing the spot size decreased the damage threshold until a spot size greater than about 150 μm was reached. Above ∿150 μm diameter, there was no spot size dependence. The result was explained on the basis of an

increased probability for hitting a defect when using a larger spot size. Diagnostics equipment were mounted rigidly either to the optical bench, steel plate, or granite rails. The diagnostic tools were of two categories: active and parametric.

Active Diagnostics

The energy and temporal shape of the laser pulse was constantly monitored by two biplanar photodiodes with S-1 photocathodes and by a calibrated pyroelectric energy meter. The temporal characteristics of the oscillator pulse were monitored by photodiode PD-1, shown in figure 6. The output of this photodiode was displayed on a Tektronix Model 519 oscilloscope and, through the first 3000 shots, was recorded for each event by a Polaroid scope camera. Due to the minute variation in this pulse shape, during the last 2800 shots only every fifth shot was so recorded.

The energy incident on target was monitored by a pyroelectric detector placed after the beam attenuating filters and before the focusing lens. It has a dynamic range from 1 joule full scale to 20 microjoules full scale. Readings as low as 5% of full scale were reliable to ±4% of full scale. Through beam splitting, attenuation at the detector head, and reflection losses, the device recorded 0.51% of the energy on target. On the two samples which exhibited the lowest threshold for damage, it was necessary to change this ratio in order to record these lower energy pulses. The detector, a Laser Precision model Rk 3230, was compared to a separate Rk 3230, and they were found to track to a precision of ±4%. The detector was calibrated against two separate carbon cone thermal calorimeters (TRG Model 117) which have an accuracy of ±10% compared to a silver sphere calorimeter. The rest of the active diagnostics were used to define the occurrence of damage.

For the purpose of this study we have defined damage as an irreversible change indicated by one of three detection techniques: (1) visible plasma formation, (2) laser induced scattering, and (3) breath-fogging.

Two observers were positioned behind 1.06 μm blocking filters at positions A and B shown on figure 6. They actively observed each event for the appearance of the bright plasma which usually accompanies the occurrence of laser-induced damage. In about 98% of the events, this observation was sufficient to positively identify damage. For the two low index materials, ZnS and ZnSe, there were several events that, even in darkened room lights, failed to produce a

visible plasma during a damaging event. In these cases a general brightening was usually observed on the surface by one or both observers. Because of the qualitative nature of this visual observation of damage, it was reinforced by the two other techniques although in the great majority of tests the detection of a plasma proved effective as a damage indicator.

The appearance of observable scatter from a He-Ne laser incident on the damage site was used as a secondary indicator. The forward scatter of He-Ne #1 at position B was used, as well as the scatter of He-Ne #2 observed at position A. Since the latter was focused on the front surface of the sample, any change in the pattern viewed on a screen placed behind position A afforded a method for distinguishing between front surface damage, back surface damage, and low lying (i.e., near the front surface) bulk damage sites. The diffraction pattern from front surface damage was quite distinctive. Although this technique proved useful in many cases, the final determination of surface damage was made by the most sensitive method, i.e., breath-fogging, which is described next.

The final technique, which proved the most sensitive, was used only after the sample was removed from the holder. It has been noted (ref. 7) that condensing water vapor on the damaged surface of an optical sample clearly indicated the extent of the damage site. It has also been noted (ref. 7) and mentioned above that the plasma associated with laser-induced damage alters the surface surrounding the damage site. During the course of this study, these two observations were tied together. Upon receipt of samples that had been ion polished, a cleaning procedure was instigated which included a one step rinsing in water. On the ion polished samples, the water would not wet the surface but beaded up and was removed readily by agitation. The phenomenon, whatever it is, must account for the efficacy of the breath-fogging technique. Plasmas associated with damaging laser irradiation, in effect, cause ion bombardment of the surface in the vicinity of the interaction zone. When one blows his breath across the sample, the first places that the condensed water vapor escapes from are the plasma polished damage sites. When viewed in oblique white light, the damage sites clearly show up. Whenever there was a doubt about whether a site had sustained damage, the fogging technique was employed. Care must be taken when employing this technique to insure that no damage testing is attempted subsequent to fogging the sample. The surface threshold is markedly reduced after the surface has been fogged. It proved to be the most sensitive of the techniques. The alteration of the surface

by the plasma appears to be permanent since samples damaged more than a year ago still reveal their sites by breath-fogging.

SECTION III
RESULTS

Internal consistency is lacking in the many published reports on laser-induced damage. One of the major causes is the many ways in which the raw data collected by the investigators is reduced to the final form. To obviate the possibility that this report will contain irreproducible results, the collection and transformation of the raw data into final form will now be discussed.

Raw Data

For this study the variables of interest included laser energy, laser pulse duration, focal spot size, and whether damage occurred on a given shot. The first and last of these have been discussed above under active diagnostics and will not be rediscussed here except to note that on each irradiation either a "damage" or a "no damage" was recorded along with the total energy incident upon the target. The focal spot size was measured using the technique described under the heading parameterization. This parameter was rechecked periodically throughout the study and was found consistent to within ±3.5%. The temporal shape of the laser pulse was recorded on a fast-sweep oscilloscope* and the pulse duration was taken as the time separation between the trace of half the maximum deflection.

Data Reduction: The energy threshold

A method for determining the energy which, for a given sample, can be reported as the energy threshold was developed. It is a method which does not rely on subjective judgement, and thus it must remove one of the largest uncertainties in experiment work. Figure 7 illustrates the method used in determining energy threshold. Each shot is represented by an energy and a +1 or -1 corresponding to damage or no damage, respectively. The highest energy event which did not cause damage is then connected with a line to the lowest energy event which did cause damage, and the energy at which the line crosses the zero axis is defined to be the energy threshold. This method removes subjective judgement from the report of the damage threshold. By effectively averaging the highest no-damage and the lowest damage the effect of either taken singly is moderated. There are those who use a similar method but report only the highest energy which did not cause damage as the threshold, but this is much more sensitive to the unusual end-point

*Tektronix Model 519

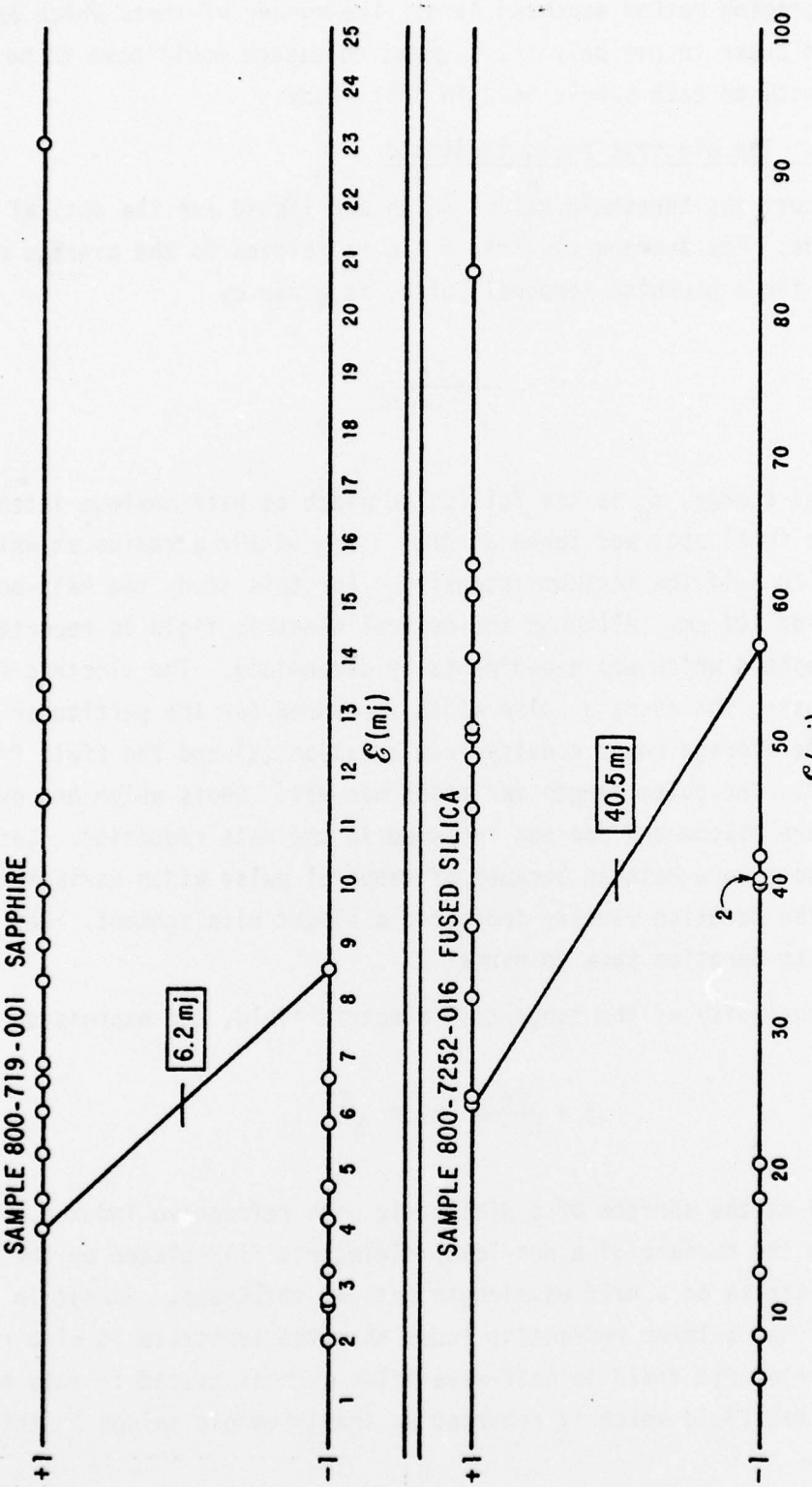

Figure 7. Method Used to Determine Energy Threshold for Damage.

than is the averaging method espoused here. The number of shots which one would need to take in order to use only the highest no-damage would have to be many times the 25 shots on each sample used in this study.

Data Reduction: The electric field threshold

In this report the threshold values which are listed are the optical electric field thresholds. The average electric field is related to the average power density which, for a gaussian temporal pulse, is given by

$$S = \frac{E}{t_p \cdot \text{area}} \tag{2}$$

where E is total energy, t_p is the full pulse width at half maximum intensity, and the area of the focal spot was taken as that lying within a radius at which the intensity fell to half the maximum intensity. For this study the half-power point had a diameter of 104 μm. Although the optical electric field is reported, it was the energy threshold which was experimentally determined. The electric field was then obtained using the average pulse width (measured for the particular sample) to calculate the average power density from equation (2) and the field from the Poynting vector. The pulse length variation was ±5%. Shots which had overly long pulse widths were discounted and not included in the data reduction. Less than 2% of the total shots were retaken because of temporal pulse width variation. Variation of the pulse duration usually indicated a slight misalignment. Realignment brought the pulse duration back to normal.

From the continuity of the tangential electric field, the expression

$$E = \frac{2n}{n+1}\ 19.4\ \sqrt{S} \tag{3}$$

gives the field at the surface of a dielectric with refractive index n. This also is the field at the surface of a non-lossy dielectric film placed on the surface in integral multiples of a half wavelength optical thickness. Except in the case in which a film has a lower refractive index than the substrate it also represents the peak electric field in half-wave films such as tested in this study. It is this calculated field which is reported as the threshold values in this report.

Data Reduction: Accuracy of results

The measured energy has an uncertainty of ±7% due to the 4% uncertainty in the pyroelectric detector and the ±5.5% uncertainty in the calorimeter used to calibrate the pyroelectric detector. The average uncertainty in threshold energy was ±19%. With a pulse width uncertainty of 5% and an uncertainty in the focal spot diameter of 3.5%, the electric field was known for a given shot to ±9.5%. Folding in the 19% for the threshold energy results in a total uncertainty in the threshold electric field of ±13.4%.

Results of the Current Study: Thin films

Surfaces of optical materials do not exhibit damage thresholds as high as their bulk values. To the author's knowledge there has been only one report which claimed that the surface and bulk thresholds of a material were measured to be the same (ref. 9). It was shown (ref. 10) that clean optical surfaces exhibited higher damage thresholds than do dirty surfaces. In fact a piece of dust on an optical surface can absorb laser radiation, and the resulting temperature rise is sufficient to cause localized damage. It was also shown (ref. 11) that particular polishing compounds containing material which is highly absorbent at the laser wavelength will lower the damage threshold. Specifically, jeweler's rouge (iron oxide) lowers the surface threshold for 1.06 μm laser wavelength even though the iron oxide is not present in sufficient quantity to be indicated by Auger spectroscopy. However, even if these two problems of dirt and particulate inclusions are scrupulously avoided, there still remains the problem of surface roughness. A major portion of an effort parallel to the one reported here (ref. 12) was concerned with the evaluation of surface roughness as it affects surface thresholds to laser-induced damage. In that study a series of fused silica samples with root mean square surface roughness varying over nearly two decades was prepared in triplicate. One of each roughness was left uncoated, one of each roughness was coated with a half wavelength thickness of SiO_2, and one of each roughness was coated with a half wavelength thickness of MgF_2. The results of that study indicated a damage behavior given by

$$\sigma^m E_{th} = \text{constant} \tag{4}$$

for the three experiments where σ is the root mean square surface roughness. The value of m was 0.61 for the uncoated samples, 0.455 for the MgF_2 coated samples, and 0.42 for the SiO_2 coated samples. In order that the intrinsic strength of several optical surfaces can be compared, it is necessary to eliminate the confusing effects of varying surface roughness. This can be done by using equation (4) to compare the threshold breakdown fields at a standard roughness. To do so, let σ_k be a standard surface roughness for a particular set of samples. Then if σ_i is the surface roughness of the i^{th} sample in the set, the threshold field for sample i, if it were to have the standard roughness σ_k, is given by

$$E^i_{th}(\sigma_k) = \left(\frac{\sigma_i}{\sigma_k}\right)^m E^i_{th}\ (\sigma_i) \tag{5}$$

In the discussion that follows m is taken as 0.5, the average of the experimentally determined values. During the course of the study (ref. 13), it was determined that for 1.06 μm radiation with 40 nsec pulse duration an equation which adequately predicts the threshold for bulk laser induced damage is given by

$$E_{th} = \frac{9.05 \times 10^3}{\sqrt{\sigma_s}\ (n^2-1)} \tag{6}$$

where σ_s is the average inter-atomic spacing in the material and n is the refractive index. Because of the dependence of threshold field on roughness given by equation (4), this expression can be used to predict threshold fields for surface damage simply by replacing σ_s by σ, the root mean square surface roughness. The comparison of thin-film thresholds with the resulting expression then reveals how nearly ideal the material in thin-film form behaves. Table 1 is a compilation of the damage threshold for five half-wavelength thick films. The experimentally observed threshold fields are compared to the threshold fields predicted for bare surfaces of the same material with a surface roughness the same as that of the thin film. The final column is the ratio of the thin-film threshold to the predicted bare-surface threshold.

Table 1.

THIN-FILM THRESHOLD VS. PREDICTED BARE-SURFACE THRESHOLD

Material	Index	σ	E_{th}(MV/cm)	$\frac{9.05 \times 10^3}{\sqrt{\sigma}\,(n^2-1)}$	Ratio
LiF	1.38	12.34	0.55	2.85	0.18
MgF_2	1.377	17.08	0.87	2.44	0.36
SiO_2	1.449	17.4	0.89	1.97	0.45
Al_2O_3	1.63/1.75	15.9	0.44	1.09	0.40
ZnSe	2.40	31.5	0.115	0.34	0.338

Here the roughness values are inferred from the scatter in the films.

The fact that a material is in film form usually relegates its threshold to a value below that of a bare surface of the same material. Films suffer from problems in adhesion, different mechanical and crystallographic properties from the bulk material, inclusions, residual stress increased and absorption, and varying degrees of inhomogeneity. Table 2 is a compilation of the ratio of thin-film to bare surface thresholds observed during this investigation. Both the thin-film and surface thresholds have been corrected for roughness to an equivalent 13.5 Å rms surface according to equation (5).

Table 2.

RATIO OF THIN-FILM TO BARE-SURFACE THRESHOLD

Material	Bare Surface Threshold (MV/cm)	Film Threshold (MV/cm)	Ratio
SiO_2 on FS	2.09	0.96	0.459
LiF on FS	3.09	0.49	0.159
MgF_2 on FS	2.78	0.98	0.35
Al_2O_3 on Sapphire	1.09	0.47	0.43
ZnSe on ZnSe	0.142	0.176	1.26

The inhomogeneous films of LiF and MgF_2 exhibit the lowest ratios. The ZnSe film is interesting in that it has a higher threshold than the bare ZnSe surface. This result is not completely unexpected due to the difficulty in producing clear, unbanded, homogeneous bulk ZnSe (ref. 14). Even though the first thought would be to never place a dielectric coating on a material, since films exhibit lower thresholds than uncoated surfaces, there are good reasons for doing so. An antireflective coating can consist of a single material, a quarter wavelength thick with index n_a, placed on a surface with refractive index n_b in which $n_a = \sqrt{n_b}$. Thus SiO_2 with index 1.449 would make a quarter-wave antireflective coating for a material with index 2.1. A typical threshold for a material with n = 2.1 is about 0.7 MV/cm for a 12.5 Å rms surface finish. Thus, SiO_2 with an experimental thin-film threshold of 0.96 MV/cm could be successfully used as an antireflective coating and may in fact increase the damage threshold of the system since the maximum field will be at the air-film interface. The same comments hold of course for any two materials in the proper ratio although many antireflective coatings are placed on materials with such low index that a suitable material is not available with the proper index to make a quarter wave antireflective coating. In such cases multilayer antireflective coatings are used. To show that the weakest layer in a multilayer coating will fail when the electric field reaches E_{th}, a series of multilayer films was subjected to laser damage.

Two types of film stacks were tested: alternating even-numbered half-wave layers of ZrO_2 and SiO_2 and alternating odd-numbered half-wave layers of ZrO_2 and SiO_2. The even-numbered series consisted of 2, 6, and 10 layers with the ZrO_2 outermost. The odd-numbered series consisted of 3, 7, 11, and 15 layers; each having ZrO_2 at the inner (i.e., on the fused silica substrate) and outer layers. Table 3 is a compilation of the data gathered on these film stacks. Here g denotes the substrate, H the high index film (ZrO_2), and L the low index film (SiO_2). In support of the field viewpoint of laser induced damage, it is the field in the ZrO_2 which is the most nearly constant. The threshold field is 0.58 MV/cm ±10.4% while the threshold energy is 4.64 mJ ±49% and the incident optical field is 0.699 MV/cm ±21.6%.

In an attempt to discover the best method of film deposition, MgF_2 films were placed on fused silica substrates by radio frequency sputtering, electron beam heating, and thermal evaporation techniques. The resultant threshold fields are given in table 4. At best the results are inconclusive . The variables involved, both those known and those unsuspected, are not well understood. The technique

Table 3.

THRESHOLD OF FILM STACKS

Design	Threshold Energy (mJ)	Incident Field (MV/cm)	Threshold Field (MV/cm)
g(LH)	9.7	1.03	0.53
$g(LH)^3$	4.53	0.70	0.62
$g(LH)^5$	3.6	0.63	0.60
gH(LH)	3.17	0.59	0.48
$gH(LH)^3$	3.5	0.62	0.58
$gH(LH)^5$	3.78	0.64	0.61
$gH(LH)^7$	4.22	0.68	0.66

Table 4.

THRESHOLDS FOR MgF_2 FILMS VS. DEPOSITION TECHNIQUE

Technique	Threshold Electric Field (MV/cm)
Electron Gun	0.737
Thermal Evaporation	0.797
R-F Sputter	0.899

which works well for one material will not necessarily produce a good film with another material.

The final result to be discussed in thin films was due to a bit of serendipity. A set of thin film samples of various materials had been prepared by electron beam heating with the angle of incidence of the coating material as the variable. When the data were analyzed, they made no sense. True, there were wide variations in surface thresholds, but there was not a clear trend with angle of incidence. The surface roughnesses of the substrates were checked but proved inadequate to resolve the discrepancies. However, while checking the absorption spectra, which are routinely run on each coating as quality control measure, an absorption peak of 1.405 μm was found to vary in direct or inverse proportions with the damage threshold, depending on the film material. A check was made which indicated that

the fused silica substrate had not all been supplied to the coating company by the same vendor. In fact the absorption peak was found to correspond to OH^- absorption and was in direct proportion to the values of OH^- concentration quoted in the vendors' literature (ref. 5). The data presented in Table 5 summarize the

Table 5.

DAMAGE THRESHOLDS FOR $\lambda/2$ FILMS VS. OH^- CONCENTRATION IN SUBSTRATE

Material	Threshold Field (MV/cm)	% T @ 1.4 μm (percent)	Angle of Vapor Incidence (deg)
Al_2O_3	0.408	90	20.3
Al_2O_3	0.391	81	29.3
Al_2O_3	0.315	90	42.0
SiO_2	1.24	83	24.96
SiO_2	1.16	85	20.3
SiO_2	0.813	92.5	42
SiO_2	0.681	93	29.3
SiO_2	0.564	94	18.55
MgF_2	0.61	95	20.3
MgF_2	0.50	85	18.55
MgF_2	0.50	85	24.96
MgF_2	0.50	86	29.3
MgF_2	0.50	86	42.0
ZrO_2	0.198	79	20.3
ZrO_2	0.252	80	42.0
ZrO_2	0.251	85	24.96
ZrO_2	0.197	86	29.3
ZrO_2	0.292	87	18.55

experimental results. The results are quite interesting, especially in the SiO_2 films; in that material, the threshold field varies directly with OH^- concentration in the substrate. This may be because SiO_2 goes onto a substrate not fully oxidized in SiO form. The additional oxidation by the OH^- of the substrate improves the film (ref. 5). Conversely in the MgF_2 films, the additional oxidation by higher OH^- concentration (seen by the lower transmission at 1.4 μm and 2.23 μm) causes the MgF_2 to deposit at least near the surface as MgO interspersed with MgF_2 (ref. 5). The trend is suggested in Al_2O_3 films for improved films by additional oxidation, and no clear relationship is evidenced by the ZrO_2 films. A definitive experiment with a controlled set of samples is obviously called for by these preliminary results.

Finally, to test whether the effects of substrate roughness could be masked by placing a thin-film coating on the surface, a set of SiO_2 and MgF_2 films were produced with substrate roughness as the variable. The experimentally determined values for the samples over-coated with half-wave thicknesses of SiO_2 are listed in table 6. Here the roughness values were measured on the uncoated surface prior

Table 6.

THRESHOLD VS. ROUGHNESS FOR THE SiO_2-OVERCOATED SAMPLES

σ(Å)	E_{th}(MV/cm)
13.75	0.89
42	0.66
82	0.42
243	0.29
335	0.24

to coating. The equation of fit is $\sigma^{0.42} E_{th} = 10.5 \pm 15\%$. It is seen that although the threshold fields are much lower than for the bare samples the relationship between threshold and roughness is preserved.

The values for the MgF_2 half-wave overcoated samples are given in table 7. The equation of fit is $\sigma^{0.46} E_{th} = 7.55 \pm 9.9\%$. Here again the threshold versus roughness relation is preserved.

Table 7.

THRESHOLD VS. ROUGHNESS FOR THE MgF_2-OVERCOATED SAMPLES

σ(Å)	E_{th}(MV/cm)
13.75	0.64
45	0.34
82	0.26
142	0.22

SECTION IV
CONCLUSIONS

The research reported here can be summarized in four major conclusions:

1. In general, thin films exhibit lower damage threshold than bare surfaces of the same material. The exception, ZnSe, is an important material for 10.6 μm wavelength applications and as such deserves further consideration as to why it is "stronger" in thin-film form than in uncoated form. The reasons for the lowered damage threshold for films may include problems with adhesion, lack of homogeneity, peculiar crystallographic structure, inclusions, film stress, and increased absorption.

2. There is a systematic and calculable variation of damage threshold as a function of material type. The predictable variation, given by equation (6), allows one to determine when optimum performance for a thin-film has been reached.

3. An identification has been made of other factors which control damage resistance of thin films. In particular the deposition technique used has some influence on the damage threshold. To a greater extent the free hydroxyl content in the substrate controls the damage threshold of certain films. Preliminary results indicate that a high OH^- concentration may produce more damage resistance films of materials such as SiO_2 and Al_2O_3. Conversely, such materials as MgF_2 and ThF_4, which are adversely affected by water vapor, will probably exhibit lower damage resistance with increasing OH^- concentration in the substrate. Thus, a material such as Cer-Vit®, which has no free OH^-, would probably make a poor substrate for oxide films but a good substrate for fluorides.

4. Finally, the most important conclusion is the antithesis of what this study was designed to prove. The substrate surface roughness is an all pervasive influence. It is not possible to quote meaningful surface damage thresholds unless the surface roughness is known. The inverse dependence of surface threshold on the square root of the roughness holds for thin films applied onto the surface. The defects of the surface of a substrate are not masked by a thin film applied to the substrate. Nor does it appear that improved surface threshold can be achieved by applying thicker films. The linear absorption in thicker films would probably decrease the damage threshold even if the substrate defects could be masked.

REFERENCES

1. Guenther, A. H., Air Force Weapons Laboratory, Kirtland Air Force Base, New Mexico, private communication.

2. Longhurst, R. S., Geometrical and Physical Optics, Jarrold and Sons, Ltd., Norwich, England, 1967.

3. Holland, L., The Properties of Glass Surfaces, Chapman and Hall, London, 1966.

4. Porteus, J. O., Theory of Surface Roughness, Journal of the Optical Society of America, 53, No. 12, 1394, December 1963.

5. Austin, R. Russel, Perkin-Elmer Optical Corporation, Norwalk, Connecticut, private communication.

6. Loomis, John S., Computing the Optical Propererties of Multilayer Coatings, AFWL-TR-75-202, Air Force Weapons Laboratory, Kirtland Air Force Base, New Mexico, 1975.

7. Bliss, E. S., and Milan, D., "Laser Induced Damage to Mirrors at Two Pulse Durations", NBS Special Publication 372, 108, 1972.

8. DeShazer, Larry G., Leung, Kang M., Newnam, Brian E., and Alyassini, Nabil, Study of Laser Irradiated Thin Films, University of Southern California, Los Angeles, California, 1973.

9. Fradin, David W., Laser Induced Damage in Solids, Harvard Univesrity, Cambridge, Massachusetts, 1973.

10. Giuliano, Concetto, R., and Hess, L. D., "Damage Threshold Studies in Ruby and Sapphire", NBS Special Publication 341, 76, 1970.

11. Putman, Joseph, Influence of Structural Effects on Laser Damage Thresholds of Discrete and Inhomogeneous Thin Films and Multilayers, Masters Thesis Submitted to the Air Force Institute of Technology, Wright-Patterson Air Force Base, Ohio, 1972.

12. House, R. A., II, The Effects of Surface Structural Properties on Laser-Induced Damage at 1.06 μm, Doctoral Dissertation Submitted to the Air Force Institute of Technology, Wright-Patterson Air Force Base, Ohio, 1972.

13. Bettis, Jerry Ray, Laser-Induced Damage as a Function of Dielectric Properties at 1.06 μm, Doctoral Dissertation Submitted to the Air Force Institute of Technology, Wright-Patterson Air Force Base, Ohio, 1975.

14. Boling, N. L., Ringlion, J. A., and Dubé, G., "Q-Switched Laser-Induced Surface Damage at 1.06 Microns", NBS Special Publication 414, 119, 1974.